



Published in final edited form as:

Nat Neurosci. 2008 October ; 11(10): 1193–1200. doi:10.1038/nn.2173.

Divergence of fMRI and neural signals in V1 during perceptual suppression in the awake monkey

Alexander Maier^{*}, Melanie Wilke^{*}, Christopher Aura^{*}, Charles Zhu[†], Frank Q. Ye[†], and David A. Leopold^{*,†}

^{*}Unit on Cognitive Neurophysiology and Imaging, Laboratory of Neuropsychology, National Institute of Mental Health, National Institutes of Health, Department of Health and Human Services, 49 Convent Dr., B2J-45, MSC 4400, Bethesda, MD 20892, USA

[†]Neurophysiology Imaging Facility, National Institute of Mental Health (NIMH), National Institute of Neurological Disorder and Stroke (NINDS), National Eye Institute (NEI), National Institutes of Health, Department of Health and Human Services, 49 Convent Dr., B2J-45, MSC 4400, Bethesda, Maryland 20892, USA

Abstract

The role of primary visual cortex (V1) in determining the contents of perception is controversial. Human functional imaging (fMRI) studies of perceptual suppression have revealed a robust drop in V1 activity when a stimulus is subjectively invisible. In contrast, monkey single unit recordings have failed to demonstrate such perception locked changes in V1. To investigate the basis of this discrepancy, we measured both the blood oxygenation level-dependent (BOLD) response and several electrophysiological signals in two behaving monkeys. We found that during conventional stimulus presentation, all signals were in good agreement, showing strong visual modulation to presentation and removal of a stimulus. However, during perceptual suppression, only the BOLD response and low frequency local field potential (LFP) signals exhibited decreases, while the spiking and high frequency LFP signals were unaffected. These results demonstrate that the coupling between the BOLD and electrophysiological signals in V1 is context dependent, with a marked dissociation occurring during perceptual suppression.

Keywords

perception; binocular rivalry; V1; fMRI; BOLD

Introduction

Perceptual suppression provides an intriguing puzzle for sensory neuroscientists: how is an unperceived stimulus represented in the brain? Binocular rivalry and related phenomena, in which salient visual patterns are rendered temporarily invisible to the observer, have been frequently employed to dissociate sensation from perception while monitoring brain activity¹. These studies have provided insight into the nature of visual suppression, but have nonetheless failed to converge on the answer to a fundamental question: namely, what role does activity in V1 play in determining the visibility of a stimulus²? The main problem is that

Correspondence to: Alexander Maier.

Author Contributions. AM, MW, and DAL designed the experiments. All authors contributed to the fMRI experiments. AM, MW and CA carried out the electrophysiological testing, MW collected the psychophysical data. AM analyzed the fMRI and electrophysiological data. AM and DAL wrote the paper.

human and animal studies have reached nearly opposite conclusions. On one hand, measurements of the blood oxygenation level-dependent (BOLD) signal in human fMRI have commonly found partial or even complete elimination of V1 responses to perceptually suppressed stimuli during rivalry^{3–9}. Those findings suggest that V1 plays a critical role in determining whether a stimulus reaches subsequent processing stages. On the other hand, monkey single-unit studies found little or no change in activity in this area as a function of perceptual state, leading to the conclusion that perceptual suppression does not involve the perturbation of visual signals in the first cortical processing stage^{10–13}. This discrepancy has been identified as a significant impediment for understanding how V1 activity contributes to perception.

Until now, it has been impossible to isolate the potential reasons for the observed differences, since fMRI and electrophysiological studies have differed in their visual stimuli, behavioral paradigms, and species tested^{3, 14, 15}. Here we directly investigate the basis of these contradictory findings, and further explore the role of V1 in visual perception, by measuring both fMRI and electrophysiological responses of two trained monkeys experiencing perceptual suppression. Using the same stimulus, behavioral paradigm, and individual monkey subjects, we report that the fMRI and neurophysiological signals, while in agreement during conventional stimulation, specifically diverge during perceptual suppression, with the fMRI signal most accurately reflecting the subjective state in primary visual cortex.

Results

The main objective of the study was to compare neural and fMRI responses under identical stimulus and perceptual conditions. To this end, we trained two monkeys to respond explicitly to the visibility of a salient target presented on a screen by depressing a lever whenever the target was present. We used the paradigm of generalized flash suppression (GFS)¹⁶, where a salient target disappears upon the abrupt onset of a surrounding field of dynamic dots, to reliably induce perceptual suppression. The stimulus sequence used in the present study is shown in (Fig. 1A). Previous work in monkeys¹³ and humans¹⁶ demonstrated that such a stimulus reliably leads to all-or-none perceptual suppression in the absence of either local or interocular conflict. By adjusting stimulus parameters, such as the density of the dots, the minimum distance between the dots and the target, and the ocular configuration, affect the probability of the all-or-none target disappearance (see **Methods**). The GFS paradigm is related to motion-induced blindness¹⁷, but has a temporal sequence that closely resembles binocular rivalry flash suppression¹⁸. Like conventional binocular rivalry, GFS suppression diminishes the visual responses of extrastriate cortical neurons, but has little effect on V1 firing rates^{10, 11, 19, 20}.

We took two general approaches to induce perceptual suppression. In the first, which we called *perceptual report* testing, we adjusted the stimulus parameters at the beginning of each session according to the monkeys' psychophysical report such that the probability of disappearance for each trial presentation was roughly 0.5. This method, which was also used in a previous study¹³, entailed the sorting of neural responses by the monkey's report on a trial-by-trial basis. The second approach, which was used to allow for direct comparison of fMRI and electrophysiological responses, was termed *block design* testing (Fig. 1B). In block design testing, used for the majority of the study, the visibility of the target was controlled throughout the each block by biasing the physical stimulus parameters (see **Methods**).

To isolate signal changes specifically related to perceptual suppression, we contrasted conditions in which the target was physically present, but rendered either visible (*VIS*) or invisible (*INV*). Because of the previously mentioned discrepancies in the literature, we were particularly interested in whether the activity level during the invisible condition would more

closely resemble the visible condition, or a control condition in which the stimulus condition was turned off when the surrounding dots appeared (*OFF*). The latter condition is indistinguishable from perceptual suppression¹⁶. For both fMRI and electrophysiological testing, brain activation was measured relative to a stimulus-free fixation condition (*FIX*). Note that the monkeys were not required to confirm the disappearance during the *block design* testing (maintaining accurate perceptual report for truly ambiguous stimuli requires a large proportion of interspersed catch trials). Nonetheless, the effectiveness of the biased stimulus configurations was evaluated repeatedly in *perceptual report* testing. The behavioral results in the two animals verify that the manipulations of stimulus visibility were highly effective (see Fig. 1C), and match the expectations of observed psychophysical results in different monkeys¹³.

In the block design, stimuli were grouped into 30s or 60s epochs of repeated 6s trials, during which the monkey was required to fixate a small cross. Blocks of the different conditions (*INV*, *VIS*, *OFF*, etc.) were presented either sequentially or in randomly interleaved order (Fig. 1B), with a total of four blocks of each type per scanning session. After successfully completed trials, the animal received a drop of apple juice and a short break (0.8–1.0s) at which point it was free to briefly move its eyes about. Two animals participated in a total of 29 fMRI sessions and 41 electrophysiology sessions, conducted over the same time period but on different days.

BOLD and spiking during perceptual suppression

We first localized the retinotopic region of V1 corresponding to the position of our recording chamber by evaluating the mapping the BOLD response to solid red disks in different positions (see **Methods**, Supp. Fig. 1). After finding the correspondence to the recording sites, we proceeded to this stimulus as a target during the different experimental conditions. Our experiments revealed that perceptual suppression of this target strongly and consistently diminished BOLD activity in the target-responsive cortex compared to the continually visible condition. Population data from two monkeys are shown in Figure 2, and reveal that the activity drops significantly during blocks of the invisible trials, where the target was physically present but perceptually suppressed, compared to blocks of visible trials, where the target was continually perceived. In fact, activity during the invisible trials was closest to the *OFF* control condition, where the target was physically removed from the screen.

Owing to the use of the block design, it was necessary to implement two distinctly different visible control conditions. Visibility was attained in one condition by binocular presentation of the target (*VIS*), and the other by reversing the temporal order of the sequence (*VIS_{TR}*). The binocular presentation of the target in the *VIS* condition explains the slightly higher response than the monocular *VIS_{TR}* condition, in agreement with previous work on binocular integration²¹. Nonetheless, this difference is small compared to the effects of perceptual suppression, where the target-responsive region showed activity that more closely resembled the effects of physically removing the stimulus. Note that in all cases, the target and surround stimuli were on for the same period of time.

Perceptual suppression was consistently observed in single sessions, and even in single voxels. It was present when the order of the stimulus blocks was sequential or randomly interleaved (see Suppl. Fig 2). These findings are consistent with a large number of human fMRI studies showing that activity in V1 reflects perceptual visibility, rather than the mere physical presence, of a stimulus^{3–9}. The data show definitively that V1 of monkeys, like that of humans, exhibits a marked drop in BOLD response activity when a visual pattern is perceptually invisible.

We next examined whether single neurons in the same fMRI-identified target representation altered their firing during perceptual suppression. We studied 172 well isolated neurons whose responses were significantly modulated by the presentation of the target (out of 318 total

neurons sampled, see **Methods**). The monkey subjects, the stimulus, and the blockdesign paradigm were identical to the fMRI testing. In sharp contrast to the modulation of the BOLD signal, neurons in the target-responsive portion of cortex showed no significant change in their mean firing during perceptual suppression (Fig. 3, t-test, $p=0.98$). Importantly, this result was found despite the excellent agreement of the spiking and the BOLD signals during the visible and invisible control blocks, when the target was physically present and absent, respectively (*VIS* and *OFF*). Thus the BOLD and spiking responses in V1, tested in the same patch of cortex in the same monkey subjects, specifically diverged during perceptual suppression. This result serves to reconcile previous single-unit studies in monkeys^{10–13} with fMRI studies in humans^{3–9} and demonstrates that neither the species nor the paradigm formed the basis of the discrepancy, but rather the nature of the measured signals themselves.

LFP modulation, perceptual suppression, and the block design

We next explored whether modulation of the local field potential signal might reflect the BOLD signal more closely than the spiking, and better match the monkey's perceptual state²². Recent work using the *perceptual report* paradigm in GFS revealed that the power of lower frequency LFP components (<30 Hz) significantly decreased when the monkey reported the disappearance of an ambiguous stimulus¹³. We thus began by investigating whether LFP modulation was present in our data by first dividing the local field potential into two frequency bands: low (5–30 Hz) and high (30–90 Hz), and then computing changes in the different bands over blocks (see Suppl. Fig. 3). We reasoned that, given the robust BOLD changes, there might be low-frequency modulation during blocks in which the target was suppressed compared to those in which it was continuously visible. In contrast to our expectations, we found no significant decrease in mean power for either the low or high frequency bands during blocks of perceptual suppression (t-test, $p=0.69$ and $p=0.68$, respectively, 95 channels). In general, we were unable to find any electrophysiological signal that, over the course of an entire block, correlated with perceptual suppression.

To explore the basis of this negative finding, we next sought to reproduce our previous findings, where the LFP had reflected perception in V1. That study used the perceptual report paradigm (in different animals), and found that purely perceptual signals were reflected in modulation of the low frequency LFP¹³. We thus trained both monkeys to report the visibility of target stimuli on trials that were all identical, but in which the target had a 0.5 probability of being suppressed (see **Methods**). In agreement with the previous results, we found clear and consistent power decreases in the low frequency LFP during suppressed trials (Suppl. Fig. 4). As a next step, we asked whether perceptual modulation had, in fact, been present in the *block design* trials, but had been diluted because of the relatively small proportion of time within the block that the target was actually suppressed. To examine this possibility, we conducted a trial-by-trial analysis of the *block design* data, beginning with a time-frequency analysis.

The spectrograms in Fig. 4A show the time course of power changes in different frequency bands within trials of different block types. We focused on the two second period following surround onset, corresponding to the period of perceptual suppression in the *INV* trials, or lack thereof in the *VIS* trials. We evaluated which frequency components were affected by suppression (*INV-VIS*), and compared the effects of suppression to those of physical removal (*OFF-VIS*). This comparison is shown in Figs. 4B and C, which plot the t-score activity changes under the two conditions. Note that the physical removal of the visual target produces a large amplitude, broadband decrease in power, but that perceptual suppression does not (see also Suppl. Fig. 5). In agreement with the perceptual report paradigm, the strongest effect of suppression was a significant decline in the power of low frequencies (orange arrow in Fig 4C), matching the result obtained from the reporting monkey described above.

The magnitude of low-frequency power modulation can be seen more clearly in Fig. 5, where data is shown for high (30–90 Hz) and low (5–30 Hz) frequency ranges, as well as spike rate, under each of the testing conditions. This analysis reveals that the perceptual suppression condition (orange) deviates significantly from the visible condition (black) in the low frequency LFP (black arrow), but that this is not the case in high frequency LFP, nor in spiking. In fact, the only detectable electrophysiological difference between the visible and invisible trials was this change in low frequency LFP power. These data are summarized in Fig. 6b, which shows the suppression index, comparing the activity change during perceptual suppression to that measured during the physical removal of the target. Of these signals, it is the BOLD and low-frequency LFP that show substantial declines relative to the control conditions, and therein reflect the state of perceptual suppression.

Discussion

These findings help to resolve a long standing discrepancy between human fMRI and monkey neurophysiology regarding the role of V1 in determining whether a stimulus is visible. The outcome of the combined fMRI/electrophysiological approach demonstrates that the different conclusions reached by human fMRI and monkey electrophysiology was due neither to species nor paradigmatic differences, but rather to the nature of the signals that were measured. While in good agreement during conventional stimulation, the BOLD and electrophysiological responses diverged markedly during perceptual suppression.

It is interesting to consider that of the signals measured, the BOLD fMRI responses, arguably the furthest removed from neural processing, provided the most reliable measure of the perceptual state, while the action potential firing rate provided the least. Why might this be the case? There are several possible explanations, some of which are discussed here. First, one cannot entirely rule out an electrophysiological sampling bias that consistently missed a subpopulation of neurons, perhaps because of their size, that carries the perceptual signal in V1 (see reference²³ for neuron-type specific modulation effects). Perceptual modulation in small, infrequently sampled neurons, such as interneurons bearing a close relationship to vascular control²⁴, might give rise to a prominent BOLD response. Another possibility is that perceptual suppression results in a temporary and spatially localized mode of cortical processing in which both inhibition and excitation are decreased, but remain in the same balance. This scenario could produce minimal or no change in the spiking of neurons, but a temporary relief of the metabolic and vascular demands, leading to a decreased hemodynamic response. It is also possible that seemingly insignificant modulatory signals distributed over a large population of neurons would escape the notice of electrophysiological analysis, but would be effectively registered in the BOLD response. Finally, it is conceivable that perceptual suppression triggers an increase in the cerebral metabolic rate of O₂ (CMRO₂) consumption that is not matched by an overcompensating increase of cerebral blood flow (CBF), leading to decreased fMRI signal during perceived target disappearance. Further experiments are required to address these and other possibilities.

A potentially attractive explanation of the present findings might be that extrageniculate input to V1 is disrupted during perceptual suppression, and that such disruption is better reflected in the BOLD changes than in neural firing. Considerable evidence suggests that synaptic activity (stemming from afferent input as well as local intra-cortical processing) might lead to BOLD responses, even in the absence of firing rate changes^{25–27}. It has long been hypothesized that recurrent activity from extrastriate areas into V1 accompanies selective attention and stimulus awareness^{28, 29}. In this context is also noteworthy that a similar mismatch between fMRI and single-unit physiology has been previously identified regarding the modulation of V1 by visual attention³⁰, suggesting that the dissociation observed here may arise in conditions other than perceptual suppression. Recent work demonstrating laminar differences in the suppressive

modulation of synaptic currents in V1³¹ holds promise for gaining a deeper understanding of both the neural mechanisms of perceptual suppression, as well as the enigmatic relationship between the fMRI signal and neural activity.

The lack of LFP power modulation over blocks of perceptual suppression was unexpected given the clear LFP power modulation with the trial-based analysis of the same data, along with the clear BOLD modulation with the block-based analysis. This result appears to indicate that the BOLD response is not a simple reflection of integrated neural activity over time, as is commonly assumed. This negative finding may owe in part to low signal-to-noise resulting from dilution over large time windows. However, it is interesting to consider that the robust suppression observed in the BOLD response is shaped by only a subset of neural events that are punctuated and context-specific. For example, neural modulation associated with the stimulus-driven events may have a proportionally stronger contribution to the hemodynamic response than do neural fluctuations occurring between trials. That would have profound implications, since there could be no unique hemodynamic transfer function to serve as a time-invariant convolution filter to translate neural and BOLD signals, as is commonly assumed. However, it is also not the case that *only* stimulus-evoked signals contribute to the fMRI signal in V1. A recent study demonstrated that endogenous neural fluctuations recorded from an electrode in this area couple tightly to the BOLD responses throughout visual cortex³².

Importantly, the present results demonstrate that the very same signals that correlate strongly with the BOLD signal in some contexts (physical stimulus removal), fail to do so in another (perceptual suppression). We found profound uncoupling of both the spiking and gamma LFP power from the BOLD response in the very same cortical tissue perceptual suppression, despite good agreement during conventional stimulus presentation. Such absence of a fixed relationship between the different neural signals is illustrated conceptually in Fig. 7. When a target stimulus eliciting a tonic neural response is physically removed (left), all measured signals are in agreement, showing corresponding decreases in amplitude. On the other hand, during perceptual suppression (right), the various responses become dissociated, and the BOLD signal no longer matches that of the neurophysiological signals. Such context dependency, as observed in the present study, might serve to explain discrepancies among previous studies investigating the relationship between BOLD, single neuron activity and LFP^{25–27, 33, 34}. Gaining a deeper understanding of the neural determinants of the BOLD fMRI signal remains a great challenge for systems neuroscience. The divergence of neural and hemodynamic signals, once understood, may eventually give mechanistic insights into brain function that neither technique alone could provide.

Methods

Subjects and testing

Two healthy adult male monkeys (*Macaca mulatta*) were used in this study. All procedures followed NIH guidelines, were approved by the Animal Care and Use Committee, and were conducted with great care for the comfort and well being of the animals. Each monkey had an MR-compatible recording well implanted over V1 which allowed for fMRI and neurophysiological testing on subsequent days. A total of 41 multielectrode recording sessions (27 and 14 sessions in monkeys CB35 and 98X009, respectively) and 29 fMRI sessions (8 and 16 sessions, respectively, as well as 5 additional sessions with randomly ordered blocks) were collected.

Stimulus and task design

All sessions were carried out while the animals were awake and performing a task, either fixation only or reporting target visibility. In the block design task, visual stimuli were

presented in 30s or 60s epochs of repeated 6s trials of a given type. Animals were required to fixate a small spot until the completion of each trial to obtain an apple juice reward. Each stimulus type consisted of a target pattern (a bright red disk, with a diameter of 4 degrees of visual angle (dva) for the majority of the experiments presented to the parafovea in one quadrant), and a surrounding field of randomly moving dots (200–500 total dots of 0.5 deg diameter, covering an area of 40×30 degrees). The random dots never approached within half a degree to the target stimulus. In the main condition (*INV*), the stimulus parameters were adjusted such that the presentation of the surround pattern resulted in perceptual suppression of the target. In two "visible" control conditions (*VIS* and *VIS_{TR}*), the parameters were adjusted such that the target almost never disappeared. In the "invisible" control condition (*OFF*), the target was physically removed from the screen upon appearance of the dots. Blocks were either presented in a repeated temporal sequence or randomly interleaved. In other testing, animals responded according to the visibility of the target by pulling a lever.

In most sessions, animals were tested in a block paradigm consisting of 60s blocks of repeated presentations of the five different stimulus types (*FIX*, *VIS_{TR}*, *VIS*, *OFF*, and *INV*). These blocks were presented either sequentially or in pseudorandom order. Within each block, the animals were required to fixate for the entire 6s presentation of a particular stimulus condition, which was repeated until the end of the block. The quality of fixation was continually monitored. Eye movements exceeding 1–2 degrees away from the fixation spot caused the trial to abort. Note that since monkeys had been trained to fixate within 0.8 degrees from the fixation spot, they kept their eyes within that region for the large majority of the time (see Suppl. Fig. 6 – Suppl. Fig. 9). Following each successful trial, the animal received a juice reward, accompanied by a short break (0.8–1 s) where the monkey was free to move its eyes about. There were typically 6–8 completed trials each minute, depending on how well the animal acquired and maintained fixation (no significant performance differences were found between the *VIS*, *VIS_{TR}*, *OFF* and *INV* condition in either animal).

We controlled for attention effects by scanning one monkey while it was still naïve to the task and thus disregarding the target stimulus as behaviorally irrelevant while the other monkey was scanned after extensive training to report perceptual disappearance of the target stimulus. No difference was found between these datasets.

Visual Stimulation

Target stimuli consisted of a monochrome disk, slowly drifting (0.25 dva/sec) or static Gabor grating patches and in some cases a circular cropped photograph of a woman's face. They were between 2 and 8 degree in size (3 degree in the most of the sessions) and presented between 2 and 10 dva away from the fixation spot in one of the four quadrants of the visual field, depending on the position of the surface coil and the selected slice package or receptive field position, respectively. Short localizer scans during which the monkey was fixating (target present versus blank screen) were performed at the beginning of most sessions in order to find the cortical region that was selectively responding to the target stimulus presentation and slice packages were adjusted to cover the corresponding region. The surround stimulus consisted of 300 to 800 randomly distributed white dots with a size of 0.5 dva that were animated to move in random direction. Monocular stimulation was achieved by fixing one of two (red and green) anaglyph filters in front of each of the monkeys' eyes and adjusting the stimulus color accordingly (see Suppl Methods for additional details).

Behavioral Paradigm

The experiments started after monkeys were performing above 95% correct in each of their tasks. Each session started with a brief calibration procedure during which the monkeys were presented with a small (0.1–0.25 dva) fixation spot at one of nine positions on the screen. After

the monkeys acquired and kept fixation for 1–3 seconds, juice reward was delivered and a new trial began. Following this procedure, we started the experimental task during which monkeys had to fixate a central spot on the screen in a 1–4 dva window for up to 10 seconds in order to receive reward (during initial training and physiology sessions in which a scleral search coil was used, the monkey was required to hold fixation in a window of 0.8 dva radius – see below). If a monkey broke fixation, the trial was aborted and reinitiated after a short delay of 100–800ms.

We performed psychophysical testing of the stimulus conditions with both monkeys in several separate test sessions outside the scanner. Stimulus disappearance was reported using custommade levers mounted inside the primate chair. One monkey had previously been trained to report the physical and subjective removal of the target stimulus using a large variety of catch trials to ensure truthful perceptual report. The other monkey was trained to do so at the end of the experimental sessions (for a more detailed description of the methods used for behavioral training and testing of GFS, see ref¹³. All parameters of the stimulation paradigm used in the RF booths were similar to those used in the scanner.

Surgery

Monkeys were implanted with posts to immobilize the head under deep isoflurane anesthesia (1.5–2%). Head restraints were machined using PEEK plastic material (McMasterCarr, Chicago, IL) and fixed to the skull using transcranial ceramic screws (Thomas Recording, Giessen, Germany) and self curing denture acrylic (Lang Inc., Wheeling, IL). In addition, scleral search coils were implanted using a standard operating procedure³⁵. Animals received antibiotics and analgesics post-operatively.

MRI Scanning

Structural and functional images were acquired in a 4.7T/60cm vertical scanner (Bruker Biospec, Ettlingen, Germany) equipped with a Siemens AC44 gradient coil (40 mT/m, <200 μ s). MR-compatible primate chairs were constructed and machined using plastic materials as well as a minimum of brass and aluminum parts. Monkeys were prevented from performing excessive jaw movements by a chin rest that was mounted to the top of the chair. Juice was delivered using an air-pressurized juicer device³⁶ through custom made brass mouth pieces. Exposure to scanner noise was reduced by means of custom formed ear plugs.

Monkeys were scanned over a period of 4 months (plus two sessions of confirmatory re-testing 12 months later) using two custom-built surface coils situated over cortical area V1. The animals had previously been acclimated to the scanner testing environment, and worked continuously for up to four hours. Electrophysiological testing was collected during the same testing period on different days using the same animals, primate chairs, stimuli, and behavioral testing parameters, in designated electrophysiology booths.

Each session began with a localizer scan in which the retinotopic area corresponding to the salient target was identified. This localizer consisted of alternating 60 blocks of trials in which the monkey was required to fixate the center of the screen and the target was presented alone, the surrounding dots were presented alone, or a fixation cross was presented alone. Following the identification of the target responsive region, we further restricted analysis to those voxels that showed significant decreases when the target was physically removed in the context of the block design (in the *OFF* condition). In all cases, significance was evaluated using multiple t-tests. Transmit-and-receive radio frequency (RF) coils had dimensions ranging from 33×33 to 37×120 mm, and were placed adjacent to the scalp of the animals before they entered the magnet bore. The size and position of the coils was optimized to achieve maximal sensitivity in the posterior portion of area V1 in the occipital lobe. At the beginning of each session, active

shimming was achieved either by manual manipulation of the gain of the shim coils, by using the FASTMAP³⁷ procedure or a combination of the two. To assess functional cortical activation, single shot gradient echo-planar imaging (GE-EPI)³⁸ sequence was used with a repetition time (TR) between 2.0 and 2.5s and an echo-time (TE) between 30 and 35 ms. Typically, between 5 and 10 axial slices were collected with a field of view (FOV) between $96 \times 113\text{mm}$ to $128 \times 128\text{mm}$ and a slice thickness of 1.25–2mm. The in-plane resolution of the functional images was $1.5 \times 1.5\text{ mm}$ for most of the scans, with an inter-slice gap between 0.05 to 0.5mm.

MR Data Analysis

All behavioral events and stimulus event times were controlled and collected using custom written software on a PC (Industrial PC, Indianapolis, IN) running the real-time operating system QNX 4 (Harman International Industries, Ottawa, Ontario, Canada). All data analysis was performed on a PC running the Windows operating system and custom written software using MATLAB (MathWorks Inc., Noci, IM) as well as the AFNI/SUMA software package³⁹. To analyze any MRI data, raw images were first converted from the generic BRUKER into the common AFNI data format. All images of a scan were then realigned to correct for motion artifacts using a custom written algorithm, and cropped to exclude any unnecessarily large region of noise from further analysis.

As a general approach to analyze functional activation, the entire set of images of each scan was converted into a time series in units of percent change by subtracting each run's mean value from the time series of each voxel, and subsequently dividing by the same value, on a voxel-by-voxel basis. Note that for presentation purposes we later subtracted the mean activity during the fixation condition from activity in the other conditions (i.e. we defined it to be our baseline to compare experimental conditions). To correct for slow drifts in the MR signal that were unrelated to the task the voxel time series of each scan were high pass filtered with bi-directional second-order Butterworth filter with a cutoff frequency of 0.0025 Hz.

Following the standard GLM approach, correlations of each voxel's MR signal and HRFconvoluted experimental time courses were computed and multiple t-tests were performed to yield slice-specific model maps of significant activity differences between conditions.

A region of interest (ROI) was defined as the target stimulus-responsive region of primary visual cortex that showed significant activity differences for target vs. non-target presentation conditions (multiple t-tests). More specifically, it was defined as any voxel within the anatomical limits of V1 with a t-value more than two standard deviations away from the average of the tscore maps (see Suppl. Fig. 1).

Neurophysiological Recordings

Extracellular single unit and local field potential recordings were carried out using both sharp insulated microelectrodes and multicontact transcortical electrodes. Single unit activity (SUA) and local field potentials (LFP) were recorded from primary visual cortex of both animals used for the fMRI experiments. Recordings were performed inside an RF-shielded booth that was also used for behavioral testing. In all cases voltages were measured against a local reference close to the electrode contacts (i.e. a stainless steel guide tube or the hypodermic metallic shaft surrounding the multicontact electrodes). Recording electrodes consisted of both single channel microelectrodes (Thomas Recording GmbH, Giessen, Germany) as well as 16- and 24-multicontact contact electrodes with an intercontact spacing of $150\mu\text{m}$ and $100\mu\text{m}$, respectively (Neurotrack Ltd, Békéscsaba, Hungary). Single unit and LFP activity was collected with both electrode types using the MAP recording system (Plexon Inc., Dallas, TX). The multicontact electrode data was further analyzed to compute the current source density.

The V1 sites were located dorsally, several millimeters posterior to the lunate sulcus, and covered the parafoveal region close to the vertical meridian. Single units were isolated and characterized in terms of their basic response characteristics using a custom-written program for receptive field estimation. Multiunit activity in the form of voltage spikes exceeding a manually set threshold were collected and digitized by the MAP recording system. Single unit impulses were derived from the multiunit data by using a commercially available spike sorting program (Plexon Inc., Dallas, TX). The quality of isolation was assessed and rated by two investigators and only units with perfectly (ie. completely unambiguous) isolated clusters were included in the analysis. The LFP (measured as voltage fluctuations between 1 Hz and 100Hz) were collected simultaneously using the same system and digitized at 1kHz. Importantly, during all recording sessions, the monkeys' task was similar in every respect to that inside the scanner. All behavioral and stimulus events were encoded and recorded together with the neuronal signal on a separate channel in order to align the data during post hoc analysis.

In one monkey (CB35), 2 recording sessions were performed with four microelectrodes (made of a 20 μm Pt₉₀W₁₀ wire with a glass coating resulting in an external diameter of 80 μm) and an impedance of 1–2 M Ω) lowered into cortex inside a 24-gauge guide tube (Thomas, Recording, Giessen, Germany) that was used to cautiously penetrate the *dura mater* using a TR Mini Matrix microdrive (Thomas Recording GmbH, Giessen, Germany) together with a MAP recording system (Plexon Inc, Dallas, TX).

All other recordings in both monkeys were performed using a 16-contact or a 24-contact electrode with an inter-contact spacing of 150 μm or 100 μm , respectively (Neurotrack Ltd, Békéscsaba, Hungary), with contact impedances varying between 0.3 and 0.5 M Ω . The multicontact electrode was manually lowered into cortex using a custom made microdrive and signals were amplified and recorded using the Plexon MAP system. We have noted that the multicontact electrode seems to bias recordings to lower layers and faster spiking neurons. Nonetheless, all of our main neurophysiological results are in line with previous studies using standard tip electrodes^{10, 12, 13}.

Recording sites in V1 were confirmed using both, neurophysiological criteria as well as anatomical MR scans. LFP were collected by band-pass filtering the extracellular voltage fluctuations of each electrode between 0.7 Hz and 170Hz (in addition to that, a 60Hz band limited filter provided by the Plexon Inc. recording software was used on some of the initial sessions).

Neuronal Data Analysis

All neurophysiological data was processed and analyzed using custom written code for MATLAB. Single unit spiking data converted into spike density functions (SDF) with a sample rate of 1 kHz, by replacing each spike time with a Gaussian kernel. LFP were re-sampled at 1 kHz and converted into microvolts as a function of time. Spectrograms were computed using the Fast Fourier Transform with a running window size of 256ms and an overlap of 255ms or the multitaper method (CHRONUX toolbox for Matlab: <http://www.chronux.org/>) using similar parameters. Both techniques yielded highly similar results.

In addition to the broadband analysis, we sub-divided the data within the frequency domain using a second order, bi-directional, zero-phase Chebyshev type-1 filter. The resulting bandlimited signals were full-wave rectified by taking their absolute value, and re-sampled at 200 Hz. Rectifying the band-limited voltage fluctuations results in a measure of time-varying amplitude, or signal power (in actuality, the square root of the power) within each frequency band. This band-limited power (BLP) is roughly equivalent to averaging several adjacent rows of a spectrogram (for an extended discussion, see⁴⁰). For conditions in which percent change

above baseline was computed, the baseline was taken to be the mean firing rate or mean band-limited LFP power measured during the fixation period.

Supplementary Material

Refer to Web version on PubMed Central for supplementary material.

Acknowledgments

Authors would like to thank G. Dold, D. Ide, N. Nichols, and T. Talbot as well as K. Smith, N. Phipps and J. Yu for technical assistance. We also thank Drs. H. Merkle for advice on the RF coils, R. Cox assistance with MR image alignment, D. Sheinberg for help with stimulus software, K. King and C. Brewer for auditory testing and earplug manufacture, W. Vinje for acquisition of multicontact electrodes, K. Tanji, A.H. Bell, Z. Saad for help with the fMRI analysis, S. Guderian and M. Schmid and K-M Mueller for discussion. Work was supported by the Intramural Research Programs of the NIMH, NINDS and NEI.

REFERENCES

1. Blake R, Logothetis NK. Visual competition. *Nat. Rev. Neurosci* 2002;3:13–21. [PubMed: 11823801]
2. Crick F, Koch C. Are we aware of neural activity in primary visual cortex? *Nature* 1995;375:121–123. [PubMed: 7753166]
3. Polonsky A, Blake R, Braun J, Heeger DJ. Neuronal activity in human primary visual cortex correlates with perception during binocular rivalry. *Nat. Neurosci* 2000;3:1153–1159. [PubMed: 11036274]
4. Tong F, Engel SA. Interocular rivalry revealed in the human cortical blindspot representation. *Nature* 2001;411:195–199. [PubMed: 11346796]
5. Haynes JD, Rees G. Predicting the stream of consciousness from activity in human visual cortex. *Curr. Biol* 2005;15:1301–1307. [PubMed: 16051174]
6. Haynes JD, Deichmann R, Rees G. Eye-specific effects of binocular rivalry in the human lateral geniculate nucleus. *Nature* 2005;438:496–499. [PubMed: 16244649]
7. Wunderlich K, Schneider KA, Kastner S. Neural correlates of binocular rivalry in the human lateral geniculate nucleus. *Nat. Neurosci* 2005;8:1595–1602. [PubMed: 16234812]
8. Lee SH, Blake R, Heeger DJ. Traveling waves of activity in primary visual cortex during binocular rivalry. *Nat. Neurosci* 2005;8:22–23. [PubMed: 15580269]
9. Lee SH, Blake R. V1 activity is reduced during binocular rivalry. *J. Vis* 2002;2:618–626. [PubMed: 12678633]
10. Leopold DA, Logothetis NK. Activity changes in early visual cortex reflect monkeys' percepts during binocular rivalry. *Nature* 1996;379:549–553. [PubMed: 8596635]
11. Leopold, DA.; Maier, A.; Wilke, M.; Logothetis, NK. Binocular rivalry and the illusion of monocular vision. In: Alais, D.; Blake, R., editors. *Binocular rivalry and perceptual ambiguity*. Cambridge, MA: MIT Press; 2004.
12. Gail A, Brinksmeyer HJ, Eckhorn R. Perception-related Modulations of Local Field Potential Power and Coherence in Primary Visual Cortex of Awake Monkey during Binocular Rivalry. *Cereb. Cortex* 2004;14:300–313. [PubMed: 14754869]
13. Wilke M, Logothetis NK, Leopold DA. Local field potential reflects perceptual suppression in monkey visual cortex. *Proc. Natl. Acad. Sci. U. S. A* 2006;103:17507–17512. [PubMed: 17088545]
14. Tong F. Primary visual cortex and visual awareness. *Nat. Rev. Neurosci* 2003;4:219–229. [PubMed: 12612634]
15. Tong F, Meng M, Blake R. Neural bases of binocular rivalry. *Trends Cogn Sci* 2006;10:502–511. [PubMed: 16997612]
16. Wilke M, Logothetis NK, Leopold DA. Generalized flash suppression of salient visual targets. *Neuron* 2003;39:1043–1052. [PubMed: 12971902]
17. Bonneh YS, Cooperman A, Sagi D. Motion-induced blindness in normal observers. *Nature* 2001;411:798–801. [PubMed: 11459058]

18. Wolfe JM. Reversing ocular dominance and suppression in a single flash. *Vision Res* 1984;24:471–478. [PubMed: 6740966]
19. Maier A, Logothetis NK, Leopold DA. Context-dependent perceptual modulation of single neurons in primate visual cortex. *Proc. Natl. Acad. Sci. U. S. A* 2007;104:5620–5625. [PubMed: 17369363]
20. Logothetis NK, Schall JD. Neuronal correlates of subjective visual perception. *Science* 1989;245:761–763. [PubMed: 2772635]
21. Gauthier C, Hoge RD. BOLD-Perfusion Coupling during Monocular and Binocular Stimulation. *Int. J. Biomed. Imaging* 2008;2008628718
22. Logothetis NK. The neural basis of the blood-oxygen-level-dependent functional magnetic resonance imaging signal. *Philos. Trans. R. Soc. Lond B Biol. Sci* 2002;357:1003–1037. [PubMed: 12217171]
23. Mitchell JF, Sundberg KA, Reynolds JH. Differential attention-dependent response modulation across cell classes in macaque visual area V4. *Neuron* 2007;55:131–141. [PubMed: 17610822]
24. Iadecola C. Neurovascular regulation in the normal brain and in Alzheimer's disease. *Nat. Rev. Neurosci* 2004;5:347–360. [PubMed: 15100718]
25. Logothetis NK. The underpinnings of the BOLD functional magnetic resonance imaging signal. *J. Neurosci* 2003;23:3963–3971. [PubMed: 12764080]
26. Niessing J, et al. Hemodynamic signals correlate tightly with synchronized gamma oscillations. *Science* 2005;309:948–951. [PubMed: 16081740]
27. Viswanathan A, Freeman RD. Neurometabolic coupling in cerebral cortex reflects synaptic more than spiking activity. *Nat. Neurosci* 2007;10:1308–1312. [PubMed: 17828254]
28. Super H, Spekreijse H, Lamme VA. Two distinct modes of sensory processing observed in monkey primary visual cortex (V1). *Nat. Neurosci* 2001;4:304–310. [PubMed: 11224548]
29. Lamme VA, Super H, Landman R, Roelfsema PR, Spekreijse H. The role of primary visual cortex (V1) in visual awareness. *Vision Res* 2000;40:1507–1521. [PubMed: 10788655]
30. Posner MI, Gilbert CD. Attention and primary visual cortex. *Proc. Natl. Acad. Sci. U. S. A* 1999;96:2585–2587. [PubMed: 10077552]
31. Maier A, Aura C, Leopold DA. Laminar differences in perceptual modulation of V1 local field potentials. *Soc. Neurosci. Abstr. Online*. 2007
32. Shmuel A, Leopold DA. Neuronal correlates of spontaneous fluctuations in fMRI signals in monkey visual cortex: Implications for functional connectivity at rest. *Human Brain Mapping*. 2008(in press)
33. Mukamel R, et al. Coupling between neuronal firing, field potentials, and FMRI in human auditory cortex. *Science* 2005;309:951–954. [PubMed: 16081741]
34. Nir Y, et al. Coupling between neuronal firing rate, gamma LFP, and BOLD fMRI is related to interneuronal correlations. *Curr. Biol* 2007;17:1275–1285. [PubMed: 17686438]
35. Judge SJ, Richmond BJ, Chu FC. Implantation of magnetic search coils for measurement of eye position: an improved method. *Vision Res* 1980;20:535–538. [PubMed: 6776685]
36. Mitz AR. A liquid-delivery device that provides precise reward control for neurophysiological and behavioral experiments. *J. Neurosci. Methods* 2005;148:19–25. [PubMed: 16168492]
37. Gruetter R. Automatic, localized *in vivo* adjustment of all first-and second-order shim coils. *Magn. Res. Med* 1993;29:804–811.
38. Mansfield P. Multi-planar image formation using NMR spin echoes. *J. Phys. C* 1977;10:L55–L58.
39. Cox RW. Software for analysis and visualization of functional magnetic resonance neuroimages. *Computers and Biomedical Research* 1996;29:162–173. [PubMed: 8812068]
40. Leopold DA, Murayama Y, Logothetis NK. Very slow activity fluctuations in monkey visual cortex: implications for functional brain imaging. *Cereb. Cortex* 2003;13:422–433. [PubMed: 12631571]

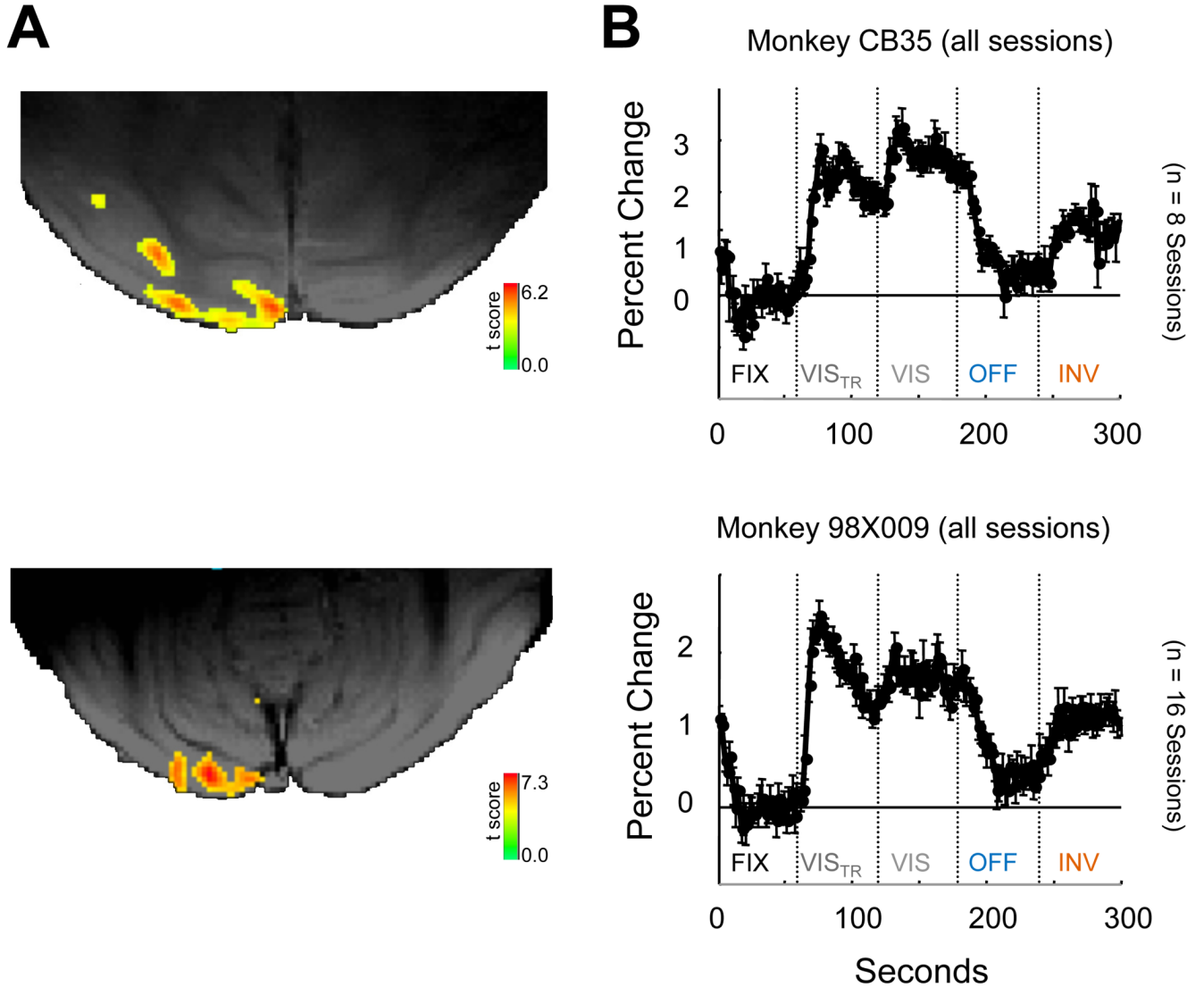
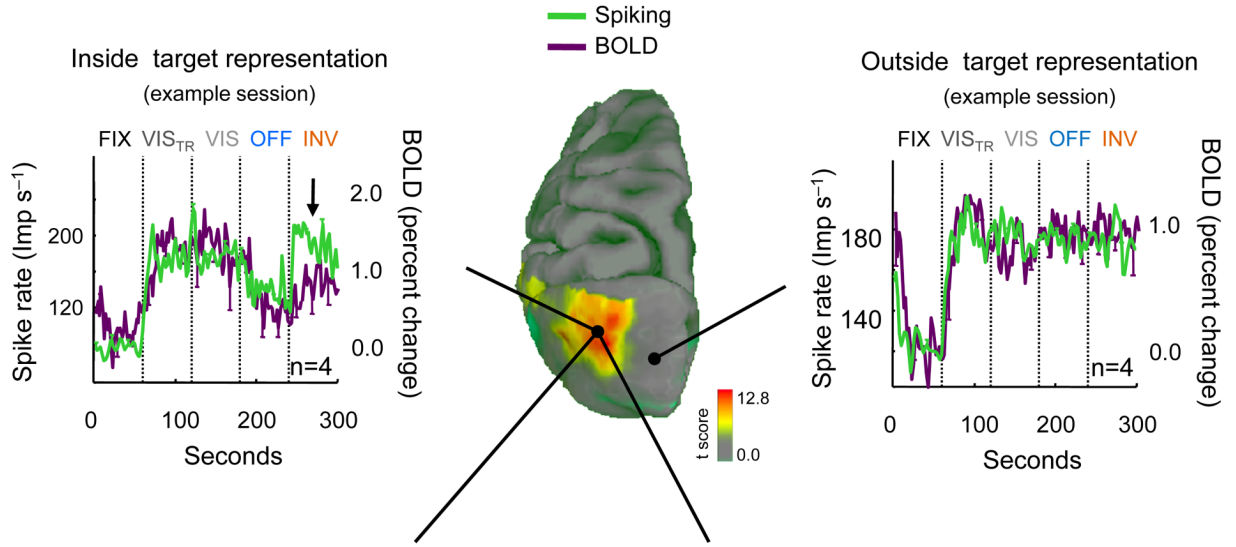


Figure 2.

Modulation of BOLD responses during perceptual suppression in two monkeys. **A.** Single-session examples of target-specific activation shown on axial slices (anterior is up, posterior down; lateral is right and medial is left). Colors represent the thresholded t-score map corresponding to the statistical comparison between four repetitions of 30s target presentation and four interleaved 30s blocks of a blank screen (see **Methods** for the parameters used for the anatomical and functional MR scans). **B.** Mean BOLD responses over all sessions in the study for both monkeys. Time course computed for those voxels showing significant decreases in activity during the *OFF* period, when the target stimulus was physically removed (see **Methods** for details). Mean + s.e.m. over 8 and 16 sessions, respectively.

A



B

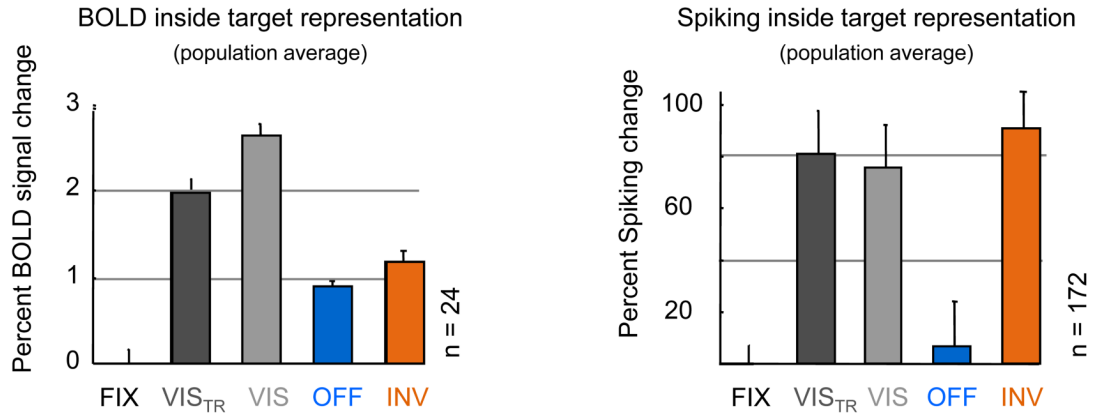


Figure 3.

Divergence of V1 single unit activity and fMRI BOLD response during perceptual suppression. **A.** Single session examples of V1 BOLD responses and single neuron firing rate inside and outside the target representation during the fMRI block design experiment. The colored region on the dorsal view of one hemisphere (anterior is up, medial is right) corresponds to the region of V1 activated by the target stimulus (data shown as t scores for a representative localizer experiment - see **Methods** and Suppl. Fig. 1). In each of the panels, activity levels for the five different stimulus conditions are shown in the sequential block paradigm (mean of 4 repetitions). Each trace represents the continuous activity level throughout 5 minutes of alternating 60s stimulation blocks consisting of up to 9 individual trials (vertical lines indicate the beginning and end of each stimulus block). Note that inside the target representation, but not outside, the BOLD and spiking activity drops in the *OFF* condition, when the target is physically removed. The spiking and fMRI signals are in close correspondence except for the GFS (*INV*) condition inside the target region. During this period, the BOLD signal shows perceptual modulation whereas the spiking activity reflects the unchanged physical. Data from monkey CB35. Each plot is mean and s.e.m. from four cycles of testing within one session. **B.** Population average across both monkeys and all experiments. The left panel depicts the mean BOLD response for all 24 scan session with time collapsed from beginning to end of each 60s block condition. Each bar represents the activation level within the ROI as a function of condition. Note the drop in BOLD during the *INV* condition where the target stimulus

became invisible. The panel on the right represents the mean firing rate of all 172 recorded targetselective neurons, expressed as %-change to baseline activity (as assessed during the *FIX* condition). The two control conditions in which the target stimulus remained visible (VIS_{TR} and *VIS*) resulted in statistically indistinguishable firing rates from the invisible (*INV*) condition (multiple t-tests, error bars represent s.e.m. between imaging sessions and neurons, accordingly).

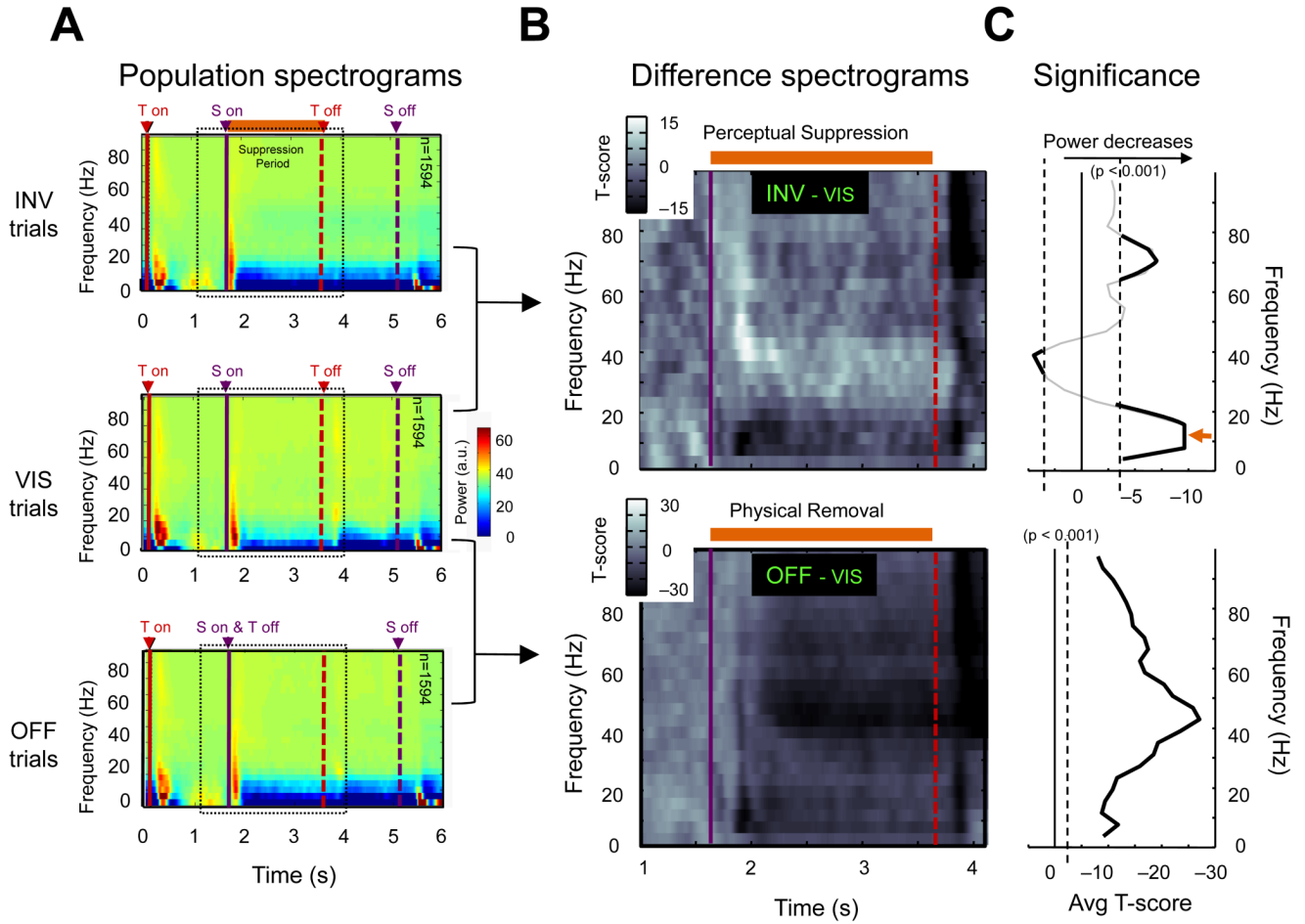


Figure 4. Spectral analysis of local field potential signals obtained during suppression and control trials. **A.** Time-frequency plots during the *INV*, *VIS* and *OFF* condition, featuring activity changes in the suppression period (following surround onset). Each panel depicts the average spectrogram for an entire trial period, with magnitude changes relative to the 500ms period preceding the surround onset, when the target alone was present in each condition. Population data is shown over all channels over all recording sessions (successfully completed trials only). All relevant stimulus events are marked with dashed lines (T = target, S = surround). Note that while all conditions showed a drop in low frequency power following the surround onset, the drop for the *INV* condition during the suppression period was larger than the corresponding drop for the *VIS* condition, but closely resembled physical removal (*OFF*). **B.** Statistical timefrequency analysis of perceptual suppression vs. physical removal (for the time period indicated by a dashed square in **A**). The upper plot (comparing the *INV* and *VIS* conditions) shows a decrease during perceptual suppression that is limited to the low frequencies, while the lower plot (comparing the *OFF* and *VIS* conditions) shows a large, broadband decrease when the target is physically removed. Note that these two conditions are nearly identical perceptually. T values are indicated by grey scale values shown in inset. **C.** Average t-score as a function of frequency for the entire period of perceptual suppression (and physical removal, accordingly). The threshold for statistical significance ($p < 0.001$) is indicated by a dashed line.

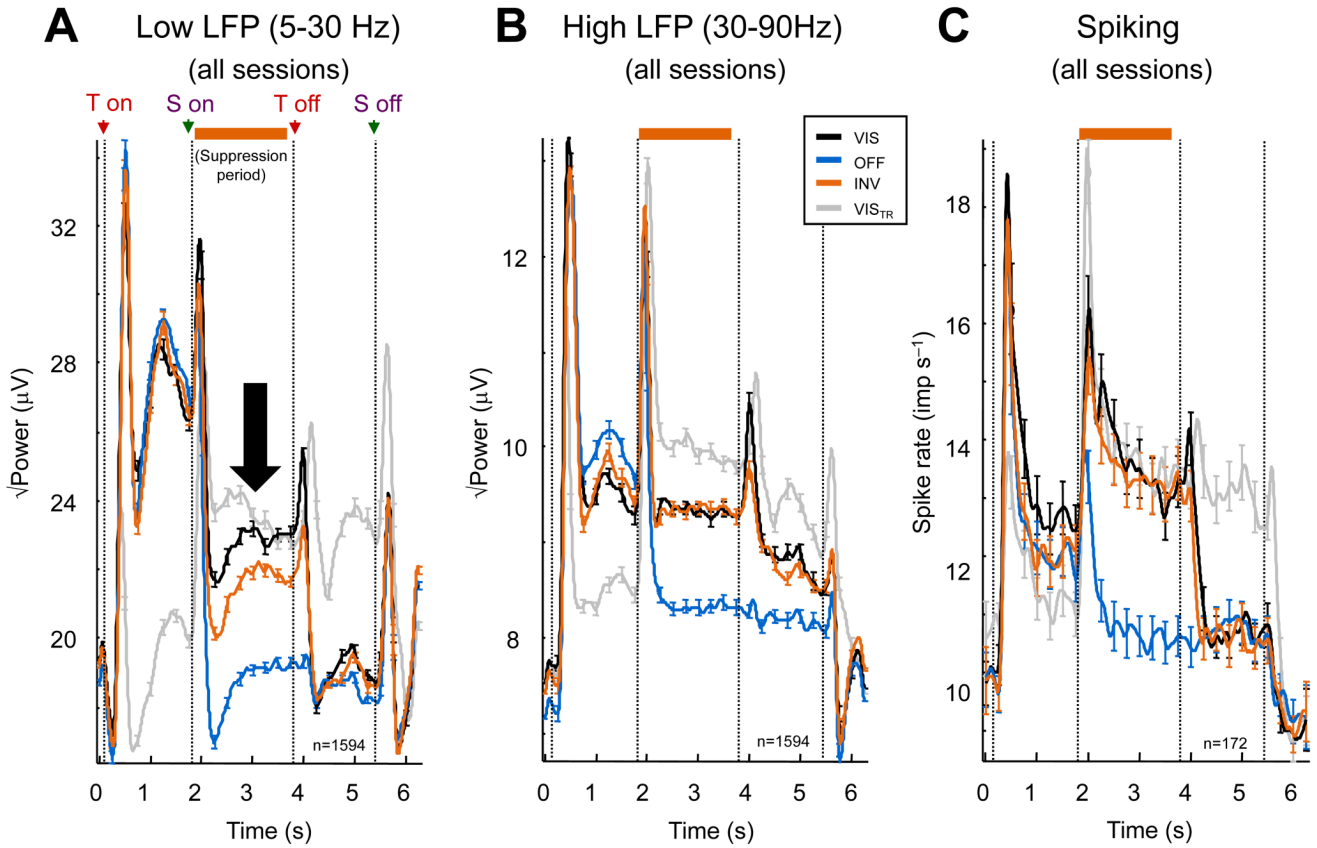


Figure 5. Population average of band limited power (BLP) and spiking time courses for different experimental conditions. **A.** Grand average of low frequency (5–30 Hz) BLP over time as a function of experimental condition (all channels recorded during all sessions with both monkeys). All relevant events are indicated with dashed lines (T = target; S = surround). The time period of interest that we focused our analysis on (during which target is perceptually suppressed during the *INV* condition) is indicated by an orange bar on top of the panel. **B.** Grand average of high frequency (30–80 Hz) BLP, same conventions as in **A.** **C.** Spiking density function of all units recorded during the neurophysiological experiments. In all cases, data are convolved with 50 ms stdev Gaussian kernel. Error bars are s.e.m. T=target, S=surround.

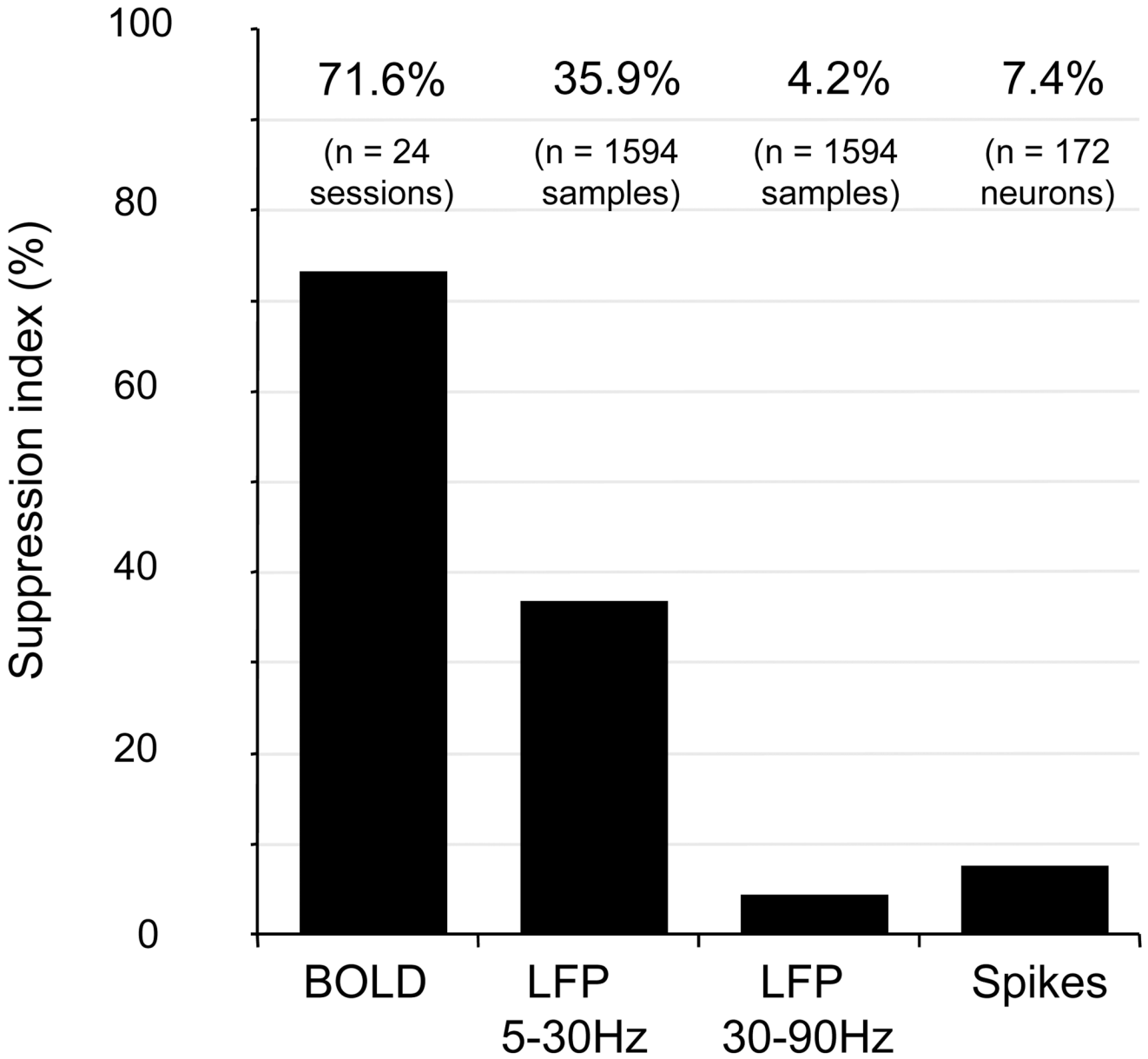


Figure 6. Summary of perceptual modulation in the BOLD and each of the electrophysiological signals (as computed from the raw data of both monkeys shown in Fig. 3B and Fig. 5). The Suppression Index corresponds to the percent of signal drop during the invisible condition (*INV*) compared to the physical removal condition (*OFF*), both relative to visible (*VIS*).

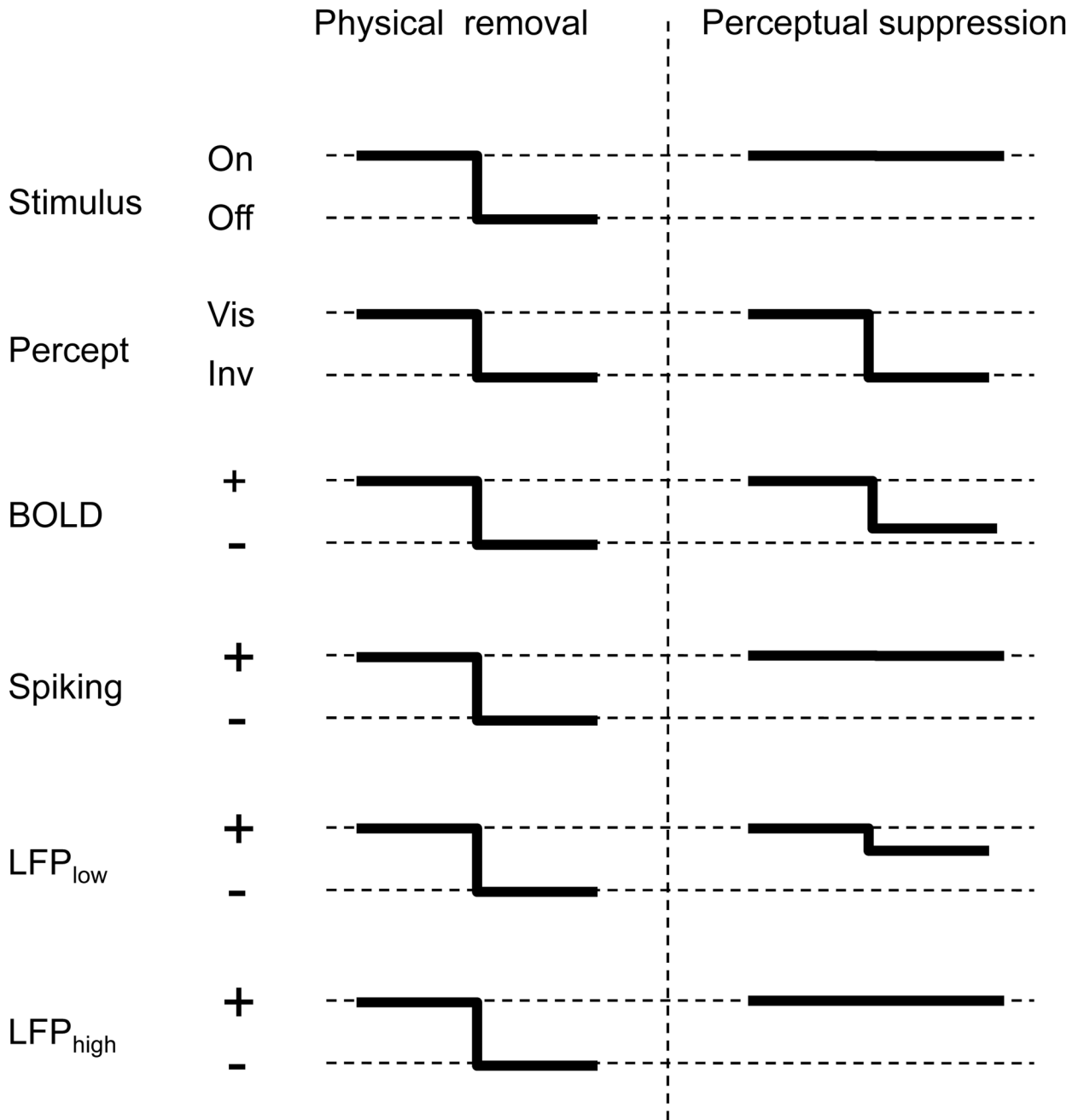


Figure 7.

Schematic illustration of main results. From top to the bottom, each line represents the state of presentation (stimulus either on or off), the reported percept of the subject (stimulus visible or invisible), as well as the various measures of neuronal activity in primary visual cortex (high or low activity). The left column represents the case where the target is physically removed from the screen (*OFF* condition). As shown in Fig. 2–Fig. 5, all measures of neuronal activity, including the fMRI BOLD response, show a decline in signal when the stimulus is both physically removed and perceptually disappears. The right hand column represents our finding for the case of perceptual suppression of the target stimulus caused by GFS (invisible condition, *INV*). Under these circumstances, the percept is dissociated from the physical stimulus in the

form of perceptual suppression. Under these conditions, the spiking activity (and high frequency LFP) maintain their activity, reflecting the continually present stimulus, while the fMRI response and (to a lesser extent) the low frequency LFP reflect the perceptual disappearance.